THE JOURNAL OF BIOLOGICAL CHEMISTRY VOL. 287, NO. 51, pp. 42867–42880, December 14, 2012

BACE1 Protein Endocytosis and Trafficking Are Differentially Regulated by Ubiquitination at Lysine 501 and the Di-leucine Motif in the Carboxyl Terminus*

Received for publication, August 2, 2012, and in revised form, October 16, 2012 Published, JBC Papers in Press, October 29, 2012, DOI 10.1074/jbc.M112.407072

Eugene L. Kang, Barbara Biscaro, Fabrizio Piazza, and Giuseppina Tesco[1]

From the Alzheimer's Disease Research Laboratory, Department of Neuroscience, Tufts University School of Medicine, Boston, Massachusetts 02111

Background: BACE1 inhibition is a primary drug target for Alzheimer disease.
Results: BACE1 endocytosis, trafficking, and degradation are differentially regulated by the di-leucine motif and ubiquitination at Lys-501 in the BACE1 carboxyl terminus.
Conclusion: BACE1 ubiquitination regulates BACE1 degradation but not its endocytosis.
Significance: Therapies able to increase BACE1 ubiquitination may represent a potential treatment for Alzheimer disease.

β-Site amyloid precursor protein-cleaving enzyme (BACE1) is a membrane-tethered member of the aspartyl proteases that has been identified as β-secretase. BACE1 is targeted through the secretory pathway to the plasma membrane and then is internalized to endosomes. Sorting of membrane proteins to the endosomes and lysosomes is regulated by the interaction of signals present in their carboxyl-terminal fragment with specific trafficking molecules. The BACE1 carboxyl-terminal fragment contains a di-leucine sorting signal (^{495}DDISLL^{500}) and a ubiquitination site at Lys-501. Here, we report that lack of ubiquitination at Lys-501 (BACE1K501R) does not affect the rate of endocytosis but produces BACE1 stabilization and accumulation of BACE1 in early and late endosomes/lysosomes as well as at the cell membrane. In contrast, the disruption of the di-leucine motif (BACE1LLAA) greatly impairs BACE1 endocytosis and produces a delayed retrograde transport of BACE1 to the trans-Golgi network (TGN) and a delayed delivery of BACE1 to the lysosomes, thus decreasing its degradation. Moreover, the combination of the lack of ubiquitination at Lys-501 and the disruption of the di-leucine motif (BACE1LLAA/KR) produces additive effects on BACE1 stabilization and defective internalization. Finally, BACE1LLAA/KR accumulates in the TGN, while its levels are decreased in EEA1-positive compartments indicating that both ubiquitination at Lys-501 and the di-leucine motif are necessary for the trafficking of BACE1 from the TGN to early endosomes. Our studies have elucidated a differential role for the di-leucine motif and ubiquitination at Lys-501 in BACE1 endocytosis, trafficking, and degradation and suggest the involvement of multiple adaptor molecules.

β-Site APP[2]-cleaving enzyme (BACE1) is a membrane-tethered member of the aspartyl proteases that has been identified as β-secretase (1–4). Sequential proteolysis of the amyloid precursor protein (APP) by β- and γ-secretase results in the production of Aβ, an ~4-kDa peptide that accumulates in the brain of subjects affected by Alzheimer disease (AD) (5). Genetic deletion of BACE1 prevents Aβ generation and reduces amyloid pathology and AD-related symptoms in AD mouse models (6–12). BACE1 null mice display a subtle phenotype consisting of transient defects in myelination that are restored later in development and behavioral alterations that are associated with the schizophrenic phenotype in humans (13–15). These phenotypes are most likely developmental in nature, and thus, BACE1 inhibition is not expected to cause significant side effects in adulthood (16). Therefore, BACE1 is a primary drug target for AD therapy. However, a decade after the discovery of β-secretase, the identification of effective BACE1 inhibitors that are active in the CNS has been very difficult. The catalytic site of BACE1 is exceptionally long, and it has been very challenging to develop small compounds that can efficiently inhibit BACE1, are able to cross the blood-brain barrier, and are reasonably stable. An alternative approach to BACE1 small molecule inhibitors is the indirect inhibition of BACE1 through the modulation of regulatory mechanisms that control BACE1 levels (17) or BACE1 trafficking to acidic compartments where it is optimally active (18).

BACE1 is targeted through the secretory pathway to the plasma membrane and is then internalized to the endosomes (19). Sorting of membrane proteins to the endosomes and lysosomes is regulated by the interaction of signals present in the carboxyl-terminal fragment (CTF) with specific trafficking molecules. Sorting signals include the di-leucine-based motifs, (DE)*XXX*L(LI) or D*XX*LL, the tyrosine-based motifs, NP*X*Y or Y*XX*∅, and ubiquitin (20). The (DE)*XXX*L(LI) motif is recognized by the adaptor protein (AP) complexes AP-1–4, whereas

* This work was supported, in whole or in part, by National Institutes of Health Grant 5R01AG025952-07 (to G. T.).
[1] To whom correspondence should be addressed: Giuseppina Tesco, Alzheimer Disease Research Laboratory, Dept. of Neuroscience, Tufts University School of Medicine, 136 Harrison Ave., Ste. 328A, Boston, MA 02111. Tel.: 617-636-4050; Fax: 617-636-2413; E-mail: Giuseppina.Tesco@Tufts.edu.
[2] The abbreviations used are: APP, β-amyloid precursor protein; BACE1, β-site APP-cleaving enzyme; AD, Alzheimer disease; Aβ, amyloid β-protein; TGN, trans-Golgi network; TSG101, tumor susceptibility gene; ESCRT, endosomal sorting complex required for transport; EGFR, epithelial growth factor receptor; HRS, hepatocyte growth factor-regulated tyrosine kinase substrate; ANOVA, analysis of variance; Tricine, *N*-[2-hydroxy-1,1-bis(hydroxymethyl)ethyl]glycine; BisTris, 2-[bis(2-hydroxyethyl)amino]-2-(hydroxymethyl)propane-1,3-diol; Ub, ubiquitin; MVB, multivesicular body; CTF, carboxyl-terminal fragment; WB, Western blot.

GGA1–3 bind to D*XX*LL via the VHS (VPS27, Hrs, andSTAM) domain. The BACE1 CTF contains a specific di-leucine sorting signal (^{495}DDISLL^{500}) (21–23). Mutagenesis of L499A/L500A (L499L500 to AA) results in retention of BACE1 at the plasma membrane (21–23) and increased protein levels following transient transfection (22). Moreover, the BACE1 acidic di-leucine motif has been shown to bind GGA1–3 (Golgi-localized γ-ear-containing ARF-binding proteins) and phosphorylation of BACE1-Ser-498 appears to increase their binding (24–28). GGA1–3 are monomeric adaptors that are recruited to the trans-Golgi network (TGN) by the Arf1-GTPase. They consist of four distinct segments: a VHS (VPS27, Hrs, and STAM) domain that binds the acidic di-leucine sorting signal D*XX*LL; a GAT (GGA and Tom1) domain that binds Arf/GTP and ubiquitin; a hinge region that recruits clathrin; and a GAE (γ-adaptin ear homology) domain that exhibits sequence similarity to the ear region of γ-adaptin and recruits a number of accessory proteins. GGAs are likely involved in the transport of proteins containing the D*XX*LL signal from the Golgi complex to the endosomes. However, several studies have shown that the GGAs bind ubiquitinated cargoes to traffic them to the lysosomes for degradation (29–33). Our previous studies have shown that BACE1 is degraded via the lysosomal pathway (23) and that depletion of GGA3 results in increased BACE1 levels and activity because of impaired lysosomal trafficking and degradation (34, 35). We recently reported that GGA3 regulates BACE1 degradation independently of the VHS/di-leucine motif interaction but requires binding to ubiquitin. We found that a GGA3 mutant with reduced ability to bind ubiquitin (GGA3L276A) is unable to regulate BACE1 levels both in rescue and overexpression experiments (35).

Originally, ubiquitination was thought to solely tag proteins for proteasomal degradation. However, it is now well established that ubiquitin is a sorting signal for membrane proteins at the TGN, plasma membrane, and endosomes to be delivered to the lysosomes (20, 36). Ubiquitin (Ub) is covalently attached to the ϵ-amino group of lysine residues of the target protein. The specificity and outcomes of ubiquitin signaling depend on the number of ubiquitin molecules (mono- or poly-ubiquitination) and the type of poly-ubiquitin chain attached to the substrate. Ubiquitination at one (mono-ubiquitination) or multiple lysines (multiubiquitination) of a target protein regulates its endocytosis and sorting to the lysosomes for degradation (37). Given that Ub contains seven lysine residues, once a molecule of Ub is attached to the target protein, additional Ub molecules can be linked to Ub resulting in the formation of polyubiquitin chains. Elongation in polyUb chains can occur at any of the seven lysine residues present in Ub. Lys-48-linked ubiquitination mainly targets proteins for proteasomal degradation. In contrast Lys-63-linked poly-ubiquitination plays a role in endocytosis and signaling functions in a proteasome-independent fashion (38). Increasing evidence is accumulating that Lys-63-linked Ub chains are a specific signal for protein sorting into the multivesicular body (MVB) pathway (39). It has recently been shown that trafficking of the yeast membrane protein Gap1 to the MVB requires both its Lys-63-linked ubiquitination and the yeast Gga GAT domain suggesting that Ggas recognize Lys-63-linked Ub chains (32). Furthermore, Ren and Hurley (40) reported that the VHS domain of Hrs, STAM, GGAs, and other trafficking molecules binds Lys-63-linked tetra-Ub chains 50-fold more tightly than monoubiquitin, although only 2-fold more than Lys-48-linked tetraubiquitin. Accordingly, we have recently determined that BACE1 is ubiquitinated at Lys-501 and is mainly mono- and Lys-63-linked poly-ubiquitinated suggesting a role for BACE1 ubiquitination in endocytosis and sorting to the lysosomes for degradation (35).

Here, we report that a BACE1 mutant resistant to ubiquitination at Lys-501 (BACE1K501R) has an increased half-life compared with BACE1 wild type (BACE1WT). However, the rate of endocytosis of BACE1K501R is similar to that of BACE1WT. In contrast, the disruption of the di-leucine motif (BACE1L499A/L500A) greatly impairs BACE1 endocytosis and the delivery of BACE1 to the lysosomes resulting in reduced BACE1 degradation. Interestingly, the combination of a lack of ubiquitination at Lys-501 and the disruption of the di-leucine motif (BACE1L499A/L500A/K501R) produces additive effects on BACE1 stabilization and defective internalization. Moreover, BACE1L499A/L500A/K501R results in BACE1 accumulation in the TGN associated with decreased levels in EEA1-positive compartments, indicating that both ubiquitination at Lys-501 and the di-leucine motif are necessary for the trafficking of BACE1 from the TGN to early endosomes.

Our studies have elucidated the role for ubiquitination at Lys-501 in endocytosis, trafficking, and degradation of BACE1. Moreover, we have determined that ubiquitination and di-leucine sorting signal differentially regulate BACE1 trafficking suggesting the involvement of multiple adaptor molecules.

EXPERIMENTAL PROCEDURES

Antibodies and Expression Vectors—The anti-V5 antibody was purchased from Invitrogen. The GAPDH antibody was purchased from Chemicon (Temecula, CA). The anti-EEA1, anti-LAMP2a, anti-TGN38, anti-calnexin, and anti-GM130 antibodies were purchased from BD Biosciences. The anti-BACE1 polyclonal antibody 7523 was a kind gift of Dr. C. Haass. PA1–757 was purchased from Affinity Bioreagents (Golden, CO). The anti-APP-CTF antibody, clone C1/6.1, was purchased from Covance (Dedham, MA). BACE1-V5 expression vector was a kind gift of Dr. B. T. Hyman (27).

Site-directed Mutagenesis, BACE1-K501R-V5, BACE1-L499A/L500A-V5, and BACE1-L499A/L500A/K501R-V5 Mutants—Site-directed mutagenesis was performed using the QuikChange site-directed mutagenesis kit (Stratagene, Santa Clara, CA) according to manufacturer's instructions. The primers used to produce each mutation are as follows: BACE1-K501R-V5 mutation (along with reverse complement primer), 5′-GACATCTCCCTGCTGAGAAAGGGCAATTCTGCAG-′3; BACE1-L499A/L500A-V5 mutation (along with reverse complement primer), 5′-GATGACATCTCCGCGGCGAAG-AAGGGCAATTC-′3; BACE1L499A/L500A/K501R-V5 mutation (along with reverse complement primer), 5′-GACATCT-CCGCGGCGAGAAAGGGCAATTCTGCAG-′3. For brevity the BACE1 wild-type and mutant constructs are referred to as BACE1WT, BACE1KR, BACE1LLAA, BACE1LLAA/KR, respectively. The resulting cDNA expression vectors were verified by sequencing.

Transient Transfection Experiments—H4-APP751 cells were seeded at a density of 250,000 per well in a 6-well plate. The following day, the cells were transfected with 0.3 μg of empty vectors or BACE1WT, BACE1KR, BACE1LLAA, BACE1LLAA/KR expression vectors using Superfect transfection reagent according to manufacturer's instructions (Qiagen, Valencia, CA). Cells were harvested 24 h post-transfection and lysed as described previously (34). Equal amounts of each sample were separated by SDS-PAGE using 4–12% BisTris gels (Invitrogen), and WB analysis was performed using anti-V5 antibody to detect BACE1 as described previously (34). GAPDH levels were detected by WB analysis with an anti-GAPDH antibody and used as a loading control. For the detection of APP-CTFs, equal amounts of each sample were separated by SDS-PAGE using 16% Tricine gels (Invitrogen).

Generation of H4 Neuroglioma Stable Cell Line Expressing BACE1-WT-V5, BACE1-K501R-V5, BACE1-L499A/L500A-V5, and BACE1-L499A/L500A/K501R-V5—H4 human neuroglioma cells expressing APP751 (H4-APP751) have been previously described (34). H4-APP751 cells were transfected with empty vector, BACE1WT, BACE1KR, BACE1LLAA, and BACE1LLAA/KR expression vectors constructs. The generation of the stable cell line was conducted as described previously (35). Isolated clones were screened for levels of BACE1 by WB analysis with anti-V5 antibody (Cell Signaling Technology, Danvers, MA) as described previously (35). For brevity, the cell lines are referred to as H4 vector, H4-BACE1WT, H4-BACE1KR, H4-BACE1LLAA, and H4-BACE1LLAA/KR, respectively.

Metabolic Labeling and Pulse-Chase Experiments—H4-BACE1WT and mutant cell lines were seeded at a density of ~45,000 cells/cm^2 in 6-well plates. Approximately 16–18 h later, they were preincubated in methionine/cysteine-free (starvation) medium for 60 min, after which they were incubated in starvation medium supplemented with 250 μCi/ml [^{35}S]methionine/cysteine (EasyTag^{TM} EXPRESS^{35}S Protein Labeling Mix, [^{35}S], PerkinElmer Life Sciences) per well for 30 min (pulse). Then cells were incubated in the presence of excess amounts of cold methionine/cysteine for indicated time points (chase). The cells were then washed, lysed in radioimmunoprecipitation assay (RIPA) Buffer (10 mM Tris, pH 8, 150 mM NaCl, 1% Nonidet P-40, 0.5% cholic acid, 0.1% SDS, 5 mM EDTA), and immunoprecipitated with an anti-V5 antibody at a concentration of 1 μg/ml (Invitrogen). Samples were separated by SDS-PAGE using 4–12% BisTris gels and MOPS running buffer (Invitrogen). Gels were fixed, dried, and exposed to a phosphorimaging screen (Bio-Rad). Images were analyzed using a Personal Molecular Imager FX and quantified using Quantity One software (Bio-Rad).

Cell Surface Biotinylation and Internalization Assay—All reagents and cells, unless otherwise stated, were kept on ice and at 4 °C. H4-BACE1WT and mutant cell lines were seeded at a density of ~35,000 cells/cm^2 in 6-well plates. Three wells were designated as "total control," "stripping control," or "internalization" for each cell line. Approximately 18–20 h later, cells were placed on ice in 4 °C room, washed twice with cold KRPH buffer (128 mM NaCl, 4.7 mM KCl, 1.25 mM $CaCl_2$ dihydrate, 1.25 mM $MgSO_4$, 5 mM Na_2HPO_4, 20 mM HEPES, pH 7.4), and incubated with KRPH buffer supplemented with 0.5 mg/ml sulfo-NHS-SS-biotin (Thermo Scientific, Rockford, IL) for 15 min at 4 °C with gentle shaking. Excess biotin was washed out with Quench Solution (KRPH buffer supplemented with 20 mM glycine) twice for 15 min. While the total control and stripping control wells were kept at 4 °C, the wells for the internalization assay were washed three times with pre-warmed growth media (1% fetal bovine serum) and incubated with pre-warmed growth media at 37 °C for 5 min. Endocytosis was stopped by quickly placing the plates on ice. Both internalization and stripping control wells were washed twice with cold KRPH. The remaining biotin at the cell surface was cleaved off by incubating stripping control and internalization wells three times in cold Cleavage Buffer (50 mM glutathione, 90 mM NaCl, 1.25 mM $CaCl_2$ dihydrate, 1.25 mM $MgSO_4$, 0.2% endotoxin-free BSA, pH 8.6) for 15 min with gentle shaking. All wells were washed twice with Quench Solution and with cold KRPH. Cells were lysed with RIPA Buffer containing protease inhibitors. Total protein was measured, and 25 μg of protein were incubated with 10 μl of streptavidin-agarose beads (Thermo Scientific, Rockford, IL) overnight with rocking at 4 °C. After washing three times with 0.5 ml of RIPA Buffer, the bound material was eluted from the beads using 2× LDS Sample Buffer (Invitrogen) containing 1.5% β-mercaptoethanol (55 °C for 10 min) and centrifuged at maximum speed for 5 min to isolate the supernatant from the beads. The supernatant containing the protein was subsequently run on a 4–12% BisTris gel using MES running buffer and probed with an anti-V5 monoclonal antibody (Invitrogen). Densitometry analysis was performed for total control, stripping control, and internalization samples. The internalization efficiency of wild-type or mutant BACE1 was calculated by the following formula: $-((\text{internalization} - \text{stripping control})/\text{total control}) \times 100$.

Immunocytochemistry—Cells stably expressing wild-type or mutated versions of BACE1 were fixed in ice-cold 4% paraformaldehyde, permeabilized, and blocked for 1 h in 10% normal goat serum containing 0.1% Triton X-100. Primary antibodies were diluted in the same medium and incubated 2 h at room temperature. Organelle localization was detected using anti-TGN38 (1:200), anti-calnexin (1:250), anti-GM130 (1:200), anti-EEA1 (1:400), and anti-LAMP2a (1:50). All antibodies were purchased from BD Transduction Laboratories. BACE1 was visualized using an antibody against its V5 tag (1:200, Bethyl Laboratories). Binding of the antibodies to their epitopes was visualized using Alexa 594-conjugated anti-mouse and Alexa 488-conjugated anti-rabbit secondary antibodies. Nuclei were counterstained by incubation with diamidino-2-phenylindole (DAPI, Sigma) for 10 min. Coverslips were washed with PBS and mounted using FluorSave (EMD Chemicals, Gibbstown, NJ).

Antibody Uptake Assay—Cells grown on polylysine-coated glass coverslips were washed twice with ice-cold PBS and incubated for 30 min on ice in serum-free medium (Opti-MEM; Invitrogen) containing the antibody 7523. Cells were then washed once with ice-cold PBS and subsequently incubated at 37 °C in complete medium for various time periods and fixed with 4% paraformaldehyde before being processed for immu-

nocytochemistry. Internalized antibodies 7523 were detected by Alexa 488-labeled anti-rabbit secondary antibody.

Confocal Microscopy and Co-localization Analysis—Two co-localization studies were performed to characterize H4 cell stably expressing either wild-type BACE1 (BACE1WT) or mutated (BACE1KR, BACE1LLAA, and BACE1LLAA/KR). Cell lines overexpressing mutated BACE1 were paired with control cell lines that were overexpressing similar levels of BACE1WT. Fifteen cells per conditions (BACE1WT1, BACE1KR, BACE1LLAA, BACE1WT2, and BACE1LLAA/KR) and antibodies (TGN38, calnexin, GM130, EEA1, and LAMP2a) were imaged for co-localization studies. Confocal microscopy was performed using Nikon A1R confocal microscope, with a ×40 objective and digital magnification. Fifteen cells per antibody and condition were imaged for both co-localization studies and the antibody uptake experiment. Co-localized pixels were quantified using the ImageJ plugin co-localization color map, which computes correlation of intensities between pairs of individual pixels in two different channels (41). For the analysis of the antibody uptake experiment, quantitative analysis was performed to measure the co-localization of BACE1 with EEA1, TGN38, or LAMP2a. This value reveals the percentage of BACE1 that reached EEA, TGN, or LAMP2a and was calculated using only the voxels for both channel 1 (green) and channel 2 (red) that had the intensities above threshold, expressed as a percentage of the total number of voxels for channel 1 above their respective thresholds. Comparisons between conditions were performed using one-way ANOVA followed by Fisher's least significant post hoc test for the first co-localization study (BACE1WT1, BACE1KR, and BACE1LLAA), and the unpaired *t* test was used for the second co-localization study (BACE1WT2 and BACE1LLAA/KR). Calculations were made with StatView 5.0.

Densitometry and Statistical Analysis—Densitometry analysis was performed on a PC computer using a LAS-4000 Fuji imaging system and Quantity One software (Bio-Rad). Values of intensity for BACE1 or APP were normalized against values of intensity of the loading control GAPDH. Statistical analysis was performed using InStat3 or StatView 5.0 software. One-way ANOVA or unpaired *t* test was employed.

RESULTS

Lack of Ubiquitination and/or Disruption of the Di-leucine Motif, within the BACE1 CTF, Results in Accumulation of BACE1 and Increased APP Processing at the β′-Site in H4 Cells—The BACE1 CTF contains both a di-leucine motif and a ubiquitination site at Lys-501 (Fig. 1*A*). We set out to determine the role of these sorting signals on BACE1 trafficking and degradation. We have previously shown that the substitution of Lys-501 to Arg (K501R) prevents BACE1 ubiquitination (35) and that mutagenesis of L499A/L500A results in BACE1 retention at the plasma membrane (23). To assess the combined effect of a lack of ubiquitination and disruption of the di-leucine motif within the BACE1 CTF, we generated a mutant BACE1 containing both L499A/L500A (BACE1LLAA) and K501R (BACE1KR) substitutions (BACE1LLAA/KR). BACE1WT and mutant constructs express a V5 tag at the carboxyl terminus. First, we tested the effect of BACE1KR, BACE1LLAA, and BACE1LLAA/KR on BACE1 steady state levels. H4-APP751 cells were transiently transfected with empty vector, BACE1WT, BACE1KR, BACE1LLAA, and BACE1LLAA/KR V5-tagged constructs. Cells were collected 24 h post-transfection. Western blot analysis with anti-V5 antibody revealed an ~4-fold increase of BACE1 levels in cells transfected with BACE1KR or BACE1LLAA compared with that expressing BACE1WT (WT *versus* KR $p < 0.001$; WT *versus* LLAA $p < 0.01$, one-way ANOVA). Interestingly, the double mutations, BACE1LLAA/KR, produced an ~8-fold increase of BACE1 levels compared with BACE1 WT and an ~2-fold increase compared with BACE1KR or BACE1LLAA (WT *versus* LLAA/KR $p < 0.001$; KR *versus* LLAA/KR $p < 0.001$; LLAA *versus* LLAA/KR $p < 0.001$, one-way ANOVA) (Fig. 1, *B* and *C*). These data indicate that both ubiquitin- and di-leucine-mediated sorting regulate BACE1 levels to a similar extent. The additive effect of the double mutation suggests that the two pathways are independent from each other.

Despite the elevation of BACE1 in the mutants, levels of secreted Aβ(1–40) were similar in the conditioned media from cells transfected with BACE1WT and mutants (data not shown). Given that the overexpression of BACE1 has been shown to promote APP processing at the β′-site resulting in the increased production of the C89 APP-CTF and +11 Aβ species (1, 5, 42), we next analyzed APP processing and found that levels of full-length APP were significantly decreased in all BACE1 mutants compared with BACE1WT or vector (WT *versus* KR, LLAA, or LLAA/KR $p < 0.001$; vector *versus* LLAA or LLAA/KR, $p < 0.001$; vector *versus* KR $p < 0.01$, one-way ANOVA) (Fig. 2, *A* and *B*). Moreover, levels of C89, normalized against the sum of C99, C89, and C83 levels, were significantly increased in all BACE1 mutants compared with BACE1WT or vector (WT *versus* KR $p < 0.01$; WT *versus* LLAA or LLAA/KR $p < 0.001$; vector *versus* WT $p < 0.01$; vector *versus* KR, LLAA, or LLAA/KR $p < 0.001$; one-way ANOVA) (Fig. 2, *C* and *D*). Levels of C99 were decreased in BACE1KR and BACE1LLAA/KR compared with BACE1WT or vector (WT *versus* KR or LLAA/KR $p < 0.05$; vector *versus* KR or LLAA/KR $p < 0.01$; one-way ANOVA) (Fig. 2, *C* and *E*). Finally, levels of C83 were decreased in all BACE1 mutants compared with BACE1WT or vector (WT *versus* KR, LLAA, or LLAA/KR $p < 0.01$; vector *versus* KR, LLAA, or LLAA/KR $p < 0.001$; one-way ANOVA) (Fig. 2, *C, E* and *F*). Altogether, these data indicate that elevation of BACE1 produced by BACE1 mutants favors APP cleavage at the β′-site resulting in increased levels of C89 and compensatory decrease of C99 and C83. Thus, although levels of secreted Aβ(1–40) are unchanged, most likely levels of +11 Aβ species are increased in the conditioned media from cells transfected with BACE1 WT and mutants.

Although the double mutations, BACE1LLAA/KR, produced an additive effect on BACE1 accumulation, APP processing was similar among all BACE1 mutants. A possible explanation for these findings is that BACE1LLAA/KR accumulates in cellular compartments where β-secretase activity is not optimal, and thus, it does not produce additive effects on APP processing.

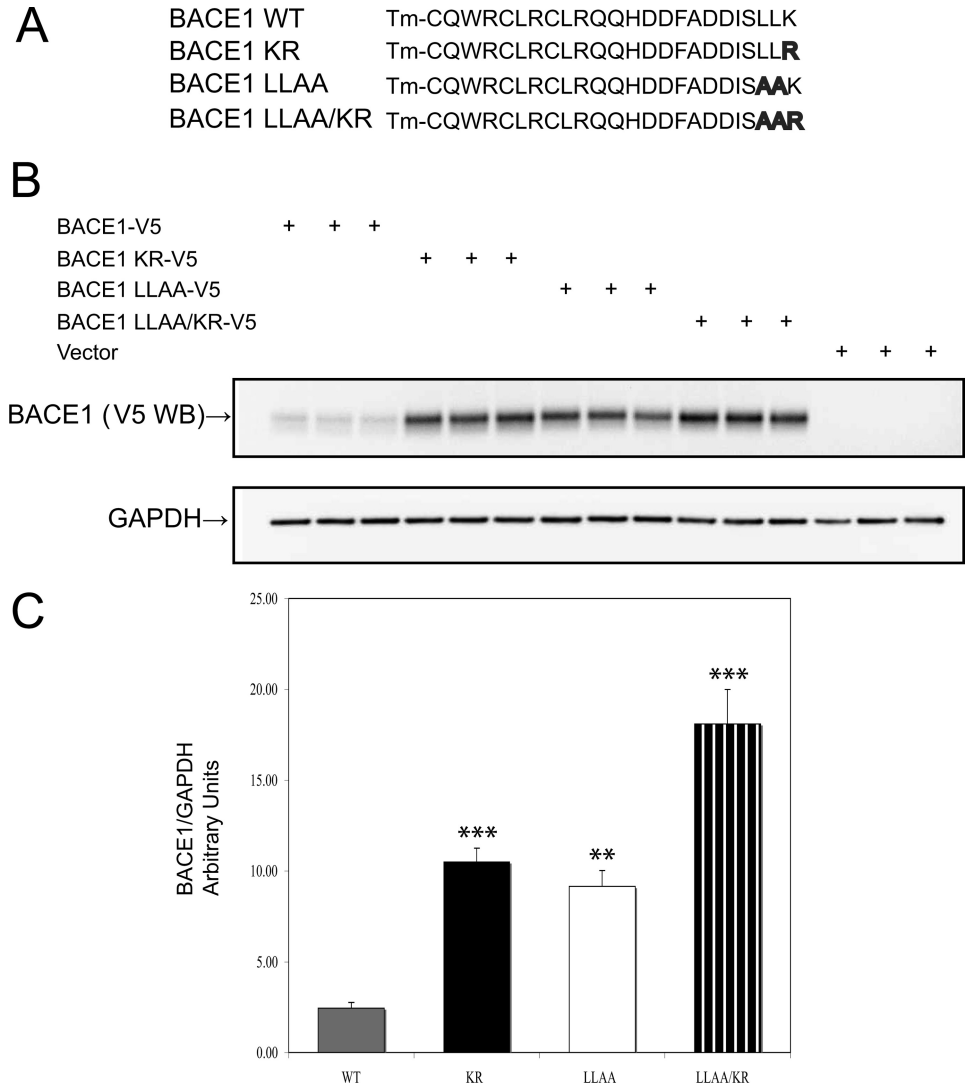

FIGURE 1. **Lack of ubiquitination and/or disruption of the di-leucine motif, within the BACE1 CTF, result in elevation of BACE1 in H4 cells.** *A,* amino acid sequences of BACE1WT and BACE1 mutants created via site-directed mutagenesis. The *2nd line* displays the substitution of lysine at position 501 with arginine, which prevents BACE1 ubiquitination. The *3rd line* displays the substitution of both leucines at position 499 and 500 with two alanines, resulting in BACE1 retention at the plasma membrane. The *4th line* shows a combination of both aforementioned mutants together. *B,* human neuroglioma (H4) cells transiently transfected with indicated expression vectors were harvested 24 h post-transfection. Levels of BACE1 and GADPH were analyzed by WB using anti-V5 and anti-GAPDH antibody, respectively. *C, graph* represents mean ± S.E. of eight BACE1 level measurements. Densitometry analysis was performed on a PC computer using a LAS-4000 Fuji imaging system and Quantity One software (Bio-Rad). BACE1 densitometry values were normalized against GAPDH values. BACE1KR and BACELLAA show significant elevation as compared with BACE1WT, whereas BACE1LLAA/KR possesses an additive effect of the two single mutants. ***, $p < 0.001$; **, $p < 0.01$, one-way ANOVA.

Ubiquitination at Lys-501 and the Carboxyl-terminal Di-leucine Motif Additively Regulate BACE1 Stability in H4 Cells—Next, we established H4-APP751 cell lines that stably express BACE1 WT and mutants. Clonal cell lines expressing similar levels of BACE1 were employed to determine the impact of KR, LLAA, or LLAA/KR mutation on the half-life of BACE1. Pulse-chase analysis revealed that KR, LLAA, or LLAA/KR mutations do not affect BACE1 maturation (Fig. 3*A*). However, the half-life of BACE1KR or LLAA mutations was increased by ~2-fold (~7.2 and ~8.5 h., respectively) compared with that of BACE1WT (~4 h). BACE1KR or LLAA levels were significantly increased compared with WT (*, $p < 0.05$; **, $p < 0.01$, respectively; one-way ANOVA) at the 6 h time point. Consistent with our finding demonstrating an additive effect of the double mutation on BACE1 steady state levels, BACE1LLAA/KR half-life (~11 h) was increased by ~3- and 1.5-fold compared with the WT or single mutations, respectively. Levels of BACE1LLAA/KR were significantly increased compared with WT at 6, 12, and 24 h (***, $p < 0.001$; **, $p < 0.01$; **, $p < 0.01$, respectively; one-way ANOVA) (Fig. 3*B*).

Lack of Ubiquitination or Disruption of the Di-leucine Motif Results in Accumulation of BACE1 in Early Endosomes—Given that both ubiquitination and the di-leucine motif regulate protein traffic, BACE1 subcellular localization was assessed by co-staining the V5 tag with a panel of markers for different organelles in H4-APP751 cell lines that stably express BACE1 WT, KR, or LLAA mutants. Confocal microscopy and co-localization studies revealed no difference in BACE1WT, BACE1KR, or BACE1LLAA localization in the TGN (TGN38) (Fig. 4, *A* and *B*, and Table 1), Golgi apparatus (GM130), or endoplas-

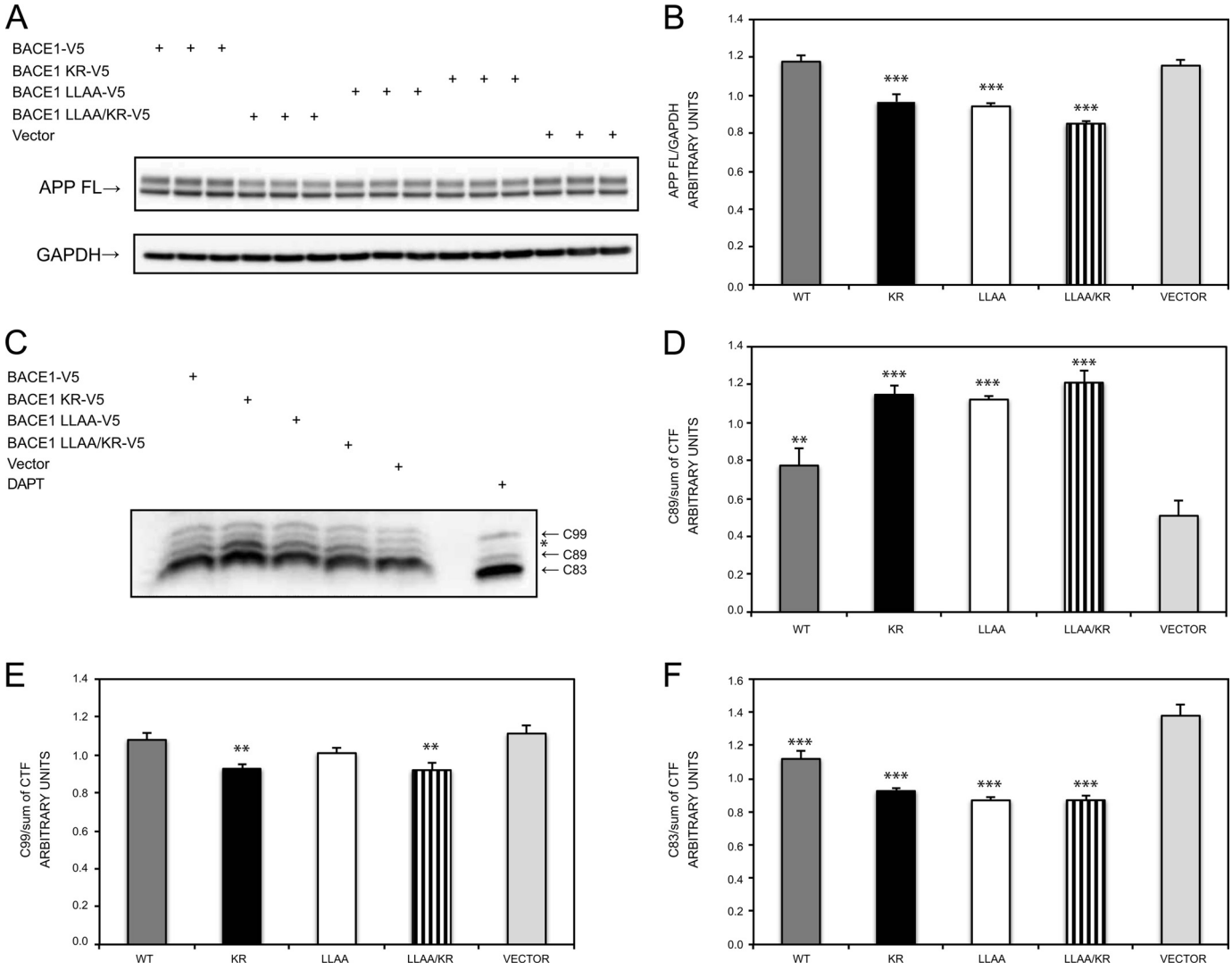

FIGURE 2. **Lack of ubiquitination and/or disruption of the di-leucine motif, within the BACE1 CTF, result in increased APP processing at the β′-site in H4 cells.** *A,* human neuroglioma (H4) cells transiently transfected with indicated expression vectors were harvested 24 h post-transfection. Levels of APP and GADPH were analyzed by WB using anti-APP CTF antibody, clone C1/6.1, and anti-GAPDH antibody, respectively. *B, graph* represents mean ± S.E. of nine full-length APP (*APP FL*) level measurements normalized against GAPDH values. *C,* APP-CTFs were detected by WB with anti-APP CTF antibody, clone C1/6.1 (16% Tricine/SDS-PAGE). H4 cells treated with 1 μM γ-secretase inhibitor, DAPT, *N*[-(3,5-difluorophenacetyl)-L-alanyl]-*S*-phenylglycine *t*-butyl ester, for 13 h, were used as a positive control for the detection of APP-CTFs. *Asterisk* indicates a faint band that is most likely nonphosphorylated C99. *D, graph* represents mean ± S.E. of nine measurements of C89 normalized against the sum of C99, C89, and C83 levels. *E, graph* represents mean ± S.E. of nine measurements of C99 normalized against the sum of C99, C89, and C83 levels. *F, graph* represents mean ± S.E. of nine measurements of C83 normalized against the sum of C99, C89, and C83 levels. Densitometry analysis was performed on a PC computer using a LAS-4000 Fuji Imaging System and Quantity One software (Bio-Rad). Ectopic expression of BACE1 mutants decreased full-length APP levels and increased C89 levels. ***, $p < 0.001$; **, $p < 0.01$, one-way ANOVA.

mic reticulum (calnexin) (Table 1). Instead, BACE1KR and BACE1LLAA accumulate in early endosomes (EEA1-positive compartments) (Fig. 4, *C* and *D*, **, $p = 0.006$ KR *versus* WT and $p = 0.05$ LLAA *versus* WT). These data indicate that both ubiquitination at Lys-501 and the di-leucine motif regulate the delivery of BACE1 to the lysosomes. Furthermore, BACE1KR also accumulates in late endosomes/lysosomes (LAMP2-positive compartments) (Fig. 4, *E* and *F*, $p = 0.03$ *versus* WT) suggesting that the ubiquitination of BACE1 is necessary for its lysosomal degradation. Our data are in agreement with previous studies showing that ubiquitination is necessary for the delivery of cell-surface proteins in the lumen of the vacuole in the MVB pathway. Accordingly, the mutagenesis of lysines in the cytosolic tails of MVB cargoes results in their accumulation at the limiting membrane of the vacuole instead of inside (43).

Lack of Ubiquitination and Disruption of the Di-leucine Motif Results in Accumulation of BACE1 in TGN and Reduction in Early Endosomes—We next determined the effect of the combined abrogation of ubiquitination and the di-leucine motif in BACE1 CTF. Subcellular localization was assessed by co-staining the V5 tag with a panel of markers for different organelles, as described above, in H4-APP751 cell lines that stably express BACE1 WT or BACE1LLAA/KR mutant. Confocal microscopy and co-localization studies revealed that BACE1LLAA/KR mutant accumulates in the TGN38 positive compartments (TGN) (**, $p = 0.0013$ WT *versus* BACE1LLAA/KR), while it is

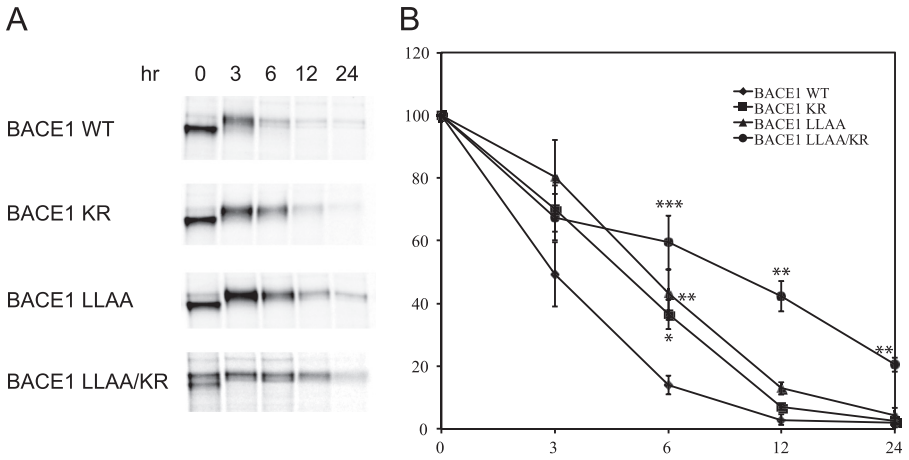

FIGURE 3. **Ubiquitination at Lys-501 and the carboxyl-terminal di-leucine motif additively regulate BACE1 stability in H4 cells.** *A,* H4-APP751 cell lines stably expressing BACE1WT-V5, BACE1LLA-V5, BACE1-V5, and BACE1LLAA/KR-V5 were metabolically labeled with [^{35}S]methionine/cysteine and harvested at indicated time points. Lysates were immunoprecipitated with anti-V5 antibody, and protein amounts were quantified by phosphorimager. *B, graph* represents the mean ± S.E. of 5–7 measurements and shows significant increases in half-life for BACE1LLAA and BACE1KR, whereas BACE1LLAA/KR shows an additive effect of both single mutants. ***, $p < 0.001$; **, $p < 0.01$, one-way ANOVA.

decreased in the EEA1-positive compartments (early endosomes) (*, $p = 0.018$ WT *versus* BACE1LLAA/KR) (Fig. 5, *A–D*). No differences were detected in the endoplasmic reticulum, Golgi apparatus, or late endosomes/lysosomes (Fig. 5, *E* and *F*, and Table 2). These data indicate that both ubiquitination at Lys-501 and di-leucine motif are necessary for trafficking BACE1 from TGN to early endosomes.

Carboxyl-terminal Di-leucine Motif but Not Ubiquitination at Lys-501 Regulates BACE1 Endocytosis—Disruption of the di-leucine motif has previously been shown to result in BACE1 accumulation at the plasma membrane (21–23, 44, 45). Moreover, we have previously shown that BACE1 is mainly mono- and Lys-63-linked poly-ubiquitinated suggesting a role for BACE1 ubiquitination in endocytosis and sorting to the lysosomes for degradation (35). Thus, we determined the effect of BACE1WT, BACE1KR, BACE1LLAA, or BACE1LLAA/KR on the rate of BACE1 endocytosis by performing cell-surface biotinylation followed by incubation at 37 °C for 5 min. Densitometry analysis of amounts of BACE1 pulled down by streptavidin beads revealed that the rate of internalization of BACE1KR was similar to that of BACE1WT. In contrast, disruption of the di-leucine motif with or without the association with mutagenesis of Lys-501 to Arg results in a dramatic defect in internalization (Fig. 6, *A* and *B*, ***, $p = 0.001$; one-way ANOVA). These data indicate that ubiquitination at Lys-501 does not regulate BACE1 internalization, whereas the di-leucine motif is the major signal controlling BACE1 endocytosis.

We next measured levels of BACE1 at the cell membrane by normalizing the amount of BACE1 pulled down at T0 without cleavage (*T*0−) against the total amount of BACE1 in the cell lysates (input) and found that all BACE1 mutants accumulate at the cell membrane, although to a different extent (~2-fold KR, ~3.5-fold LLAA, and ~5-fold LLAA/KR *versus* WT) (Fig. 6, *C* and *D*).

Lack of Ubiquitination Results in Accumulation of BACE1 in Early Endosomes and Lysosomes Following Endocytosis—Next, we determined the role of BACE1 ubiquitination at Lys-501 in the trafficking of BACE1 from the cell membrane to the endosomal/lysosomal compartment and retrograde transport to the TGN by performing a pulse-chase antibody uptake assay with an antibody raised against the amino terminus of BACE1 (24) in cell lines expressing BACE1WT or BACE1KR mutant. BACE1 staining at *T*0 (no internalization) revealed a discrete accumulation of BACE1KR in puncta adjacent to the cell membrane (Fig. 7, *A*, *C,* and *D*). Then BACE1 internalization was allowed by incubating cells at 37 °C for various intervals of time. To identify the different subcellular compartments, cells were co-stained with markers for early endosomes (EEA1), late endosomes/lysosomes (LAMP2), and TGN (TGN38). The percentage of BACE1 delivered from the cell membrane to early and late endosomes, lysosomes, or TGN at each time point was calculated by quantitative analysis of BACE1 co-localization with each organelle marker. The percentage of BACE1KR in EEA1-positive compartments was significantly increased compared with BACE1WT after 15 and 30 min of internalization (Fig. 7, *A* and *B*, and Table 3). BACE1KR also accumulates in LAMP2-positive compartments starting at *T*30 min and remains elevated up to 180 min post-internalization (Fig. 7, *C* and *D*, and Table 4). In contrast, lack of ubiquitination at Lys-501 does not affect BACE1 retrograde transport to the TGN (Fig. 7, *E* and *F*, and Table 5). The accumulation in EEA1-positive compartment is most likely caused by the impaired trafficking to the lysosomes and decreased degradation of the BACE1KR mutant (Fig. 3, *A* and *B*).

Disruption of Di-leucine Motif Delays Trafficking to Early and Late Endosomes/Lysosomes and Retrotransport to TGN Following Endocytosis—In the same sets of experiments, we also investigated the effect of BACE1LLAA and BACE1LLAA/KR mutant on BACE1 trafficking following internalization. Consistent with the biotinylation assay (Fig. 6, *C* and *D*), BACE1LLAA and BACE1LLAA/KR are clearly retained at the cell membrane (Fig. 7, *A*, *C,* and *E*, *T0*). Moreover, BACE1LLAA and BACE1LLAA/KR accumulate in early endosomes after 30 and 180 min of internalization, respectively (Fig. 7, *A* and *B*, and Table 3), and LAMP2-positive compartments after 180 min of internalization (Fig. 7, *C* and *D*, and

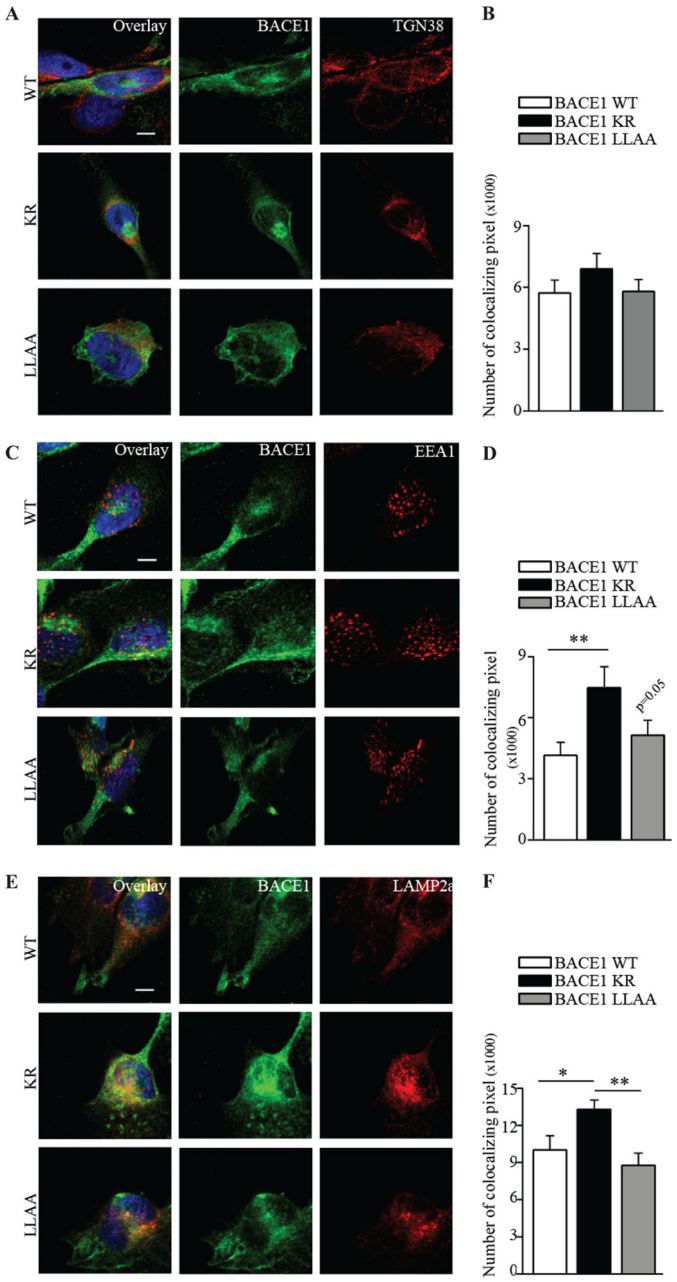

FIGURE 4. **Lack of ubiquitination or disruption of the di-leucine motif results in accumulation of BACE1 in early endosomes.** All *bar graphs* represent mean values of co-localizing pixels ± S.E. (**, $p < 0.001$; *, $p < 0.05$, one-way ANOVA), *scale bar*, 5 μm. *A*, representative photomicrographs of stable cell lines for BACE1WT (*upper lane*), BACE1KR (*middle lane*), and BACE1LLAA (*lower lane*) stained with the trans-Golgi network marker TGN38. *B, bar graph* shows no significant difference in TGN localization of BACE1WT, BACE1KR, or BACE1LLAA. *C*, representative photomicrographs of the same stable cell lines stained with the early endosomes marker EEA1. *D, bar graph* shows accumulation of BACE1KR and BACE1LLAA in the early endosomes. *E*, representative photomicrographs of the same stable cell lines stained with the late endosomes/lysosomes marker LAMP2. *F, bar graph* shows accumulation of BACE1KR in late endosomes/lysosomes.

Table 4). Both LLAA and LLAA/KR result in a delayed delivery of BACE1 to the TGN as revealed by accumulation of both mutants after 180 min of internalization (Fig. 7, *E* and *F*, and Table 5). Most likely, the accumulation of BACE1LLAA and LLAA/KR mutants in early endosomes is caused by decreased degradation in a similar fashion to the BACE1KR mutant. However, the di-leucine motif seems to play a critical role in targeting BACE1 to the lysosomes.

DISCUSSION

Our studies have elucidated a differential role of two sorting signals in BACE1 CTF, the di-leucine motif, and ubiquitination at Lys-501 in BACE1 endocytosis, trafficking, and degradation (Fig. 8*A*).

Here, we report that lack of ubiquitination at Lys-501 (BACE1KR) does not affect the rate of endocytosis but increases levels of BACE1 because of its stabilization. As a consequence, BACE1 accumulates in early and late endosomes/lysosomes and at the cell membrane (Fig. 8*B*). Next, we confirmed and extended previous findings by showing that the disruption of the di-leucine motif (BACE1LLAA) greatly impairs BACE1 endocytosis, resulting in BACE1 accumulation at the cell membrane, and it increases the steady state levels of BACE1 following transient transfection. Then we determined that disruption of the di-leucine motif produces a delayed retrograde transport of BACE1 to the TGN as well as delayed delivery of BACE1 to the lysosomes impairing BACE1 degradation (Fig. 8*C*). Interestingly, the combination of the lack of ubiquitination at Lys-501 and the disruption of the di-leucine motif (BACE1LLAA/KR) produces an accumulation of BACE1 in the TGN, while its levels are decreased in EEA1-positive compartments suggesting that the transport of BACE1 from the TGN to the endosomes is interrupted (Fig. 8*D*). Levels of BACE1LLAA/KR at the cell membrane are increased compared with the LLAA single mutant most likely because of the direct delivery of BACE1 at the cell membrane (bypassing the endosomes) in association with defective internalization. These data indicate that both ubiquitination at Lys-501 and the di-leucine motif are necessary for the trafficking of BACE1 from the TGN to early endosomes. The lack of ubiquitination seems to be compensated by the presence of the di-leucine motif and vice versa in the single mutants. Thus, the KR and LLAA mutants do not accumulate in the TGN. However, it is possible that in the presence of the KR or LLAA mutations, an increased amount of BACE1 is transported directly to the cell membrane and escapes the endosomes (Fig. 8, *B* and *C*). This model can provide an explanation for the accumulation of the KR mutant at the cell membrane in the absence of defective internalization. An alternative explanation is that the defective degradation of BACE1KR results in its accumulation in several cellular compartments, including the cell membrane. Furthermore, the double mutation produces additive effects on BACE1 stabilization indicating that both signals regulate the delivery of BACE1 to the lysosomes. Altogether, these findings indicate that BACE1 trafficking is regulated by multiple adaptor molecules.

GGA1–3 have been shown to bind to the BACE1 ^{496}DISLL^{500} motif via their VHS domain, and the phosphorylation of BACE1-Ser-498 appears to increase this binding (24–28). GGA1, moreover, has been shown to regulate the retrograde transport of BACE1 from the endosome to the trans-Golgi network (26). RNAi-mediated depletion of GGA1, 2, or 3 results in BACE1 accumulation in early endosomes (44). GGAs are likely involved in the transport of proteins containing the D*XX*LL signal from the Golgi complex to the endosomes. However,

TABLE 1

Percentage of BACE1 in different subcellular compartments

Values represent average numbers of co-localizing pixels ± S.E. NS means not significant.

	BACE1WT1	BACE1KR	BACE1LLAA	Statistics
TGN38	5721 ± 629	6888 ± 751	5788 ± 595	NS
Calnexin	8267 ± 956	10221 ± 1090	10819 ± 1300	NS
GM130	4448 ± 680	5746 ± 860	5975 ± 535	NS
EEA1	4143 ± 648	7464 ± 1024**	5143 ± 725*	**, $p = 0.006$ *versus* WT; *, $p = 0.05$ *versus* WT
LAMP2	10009 ± 1142	13267 ± 736*	8746 ± 1023**	*, $p = 0.03$ *versus* WT; **, $p = 0.003$ *versus* LLAA

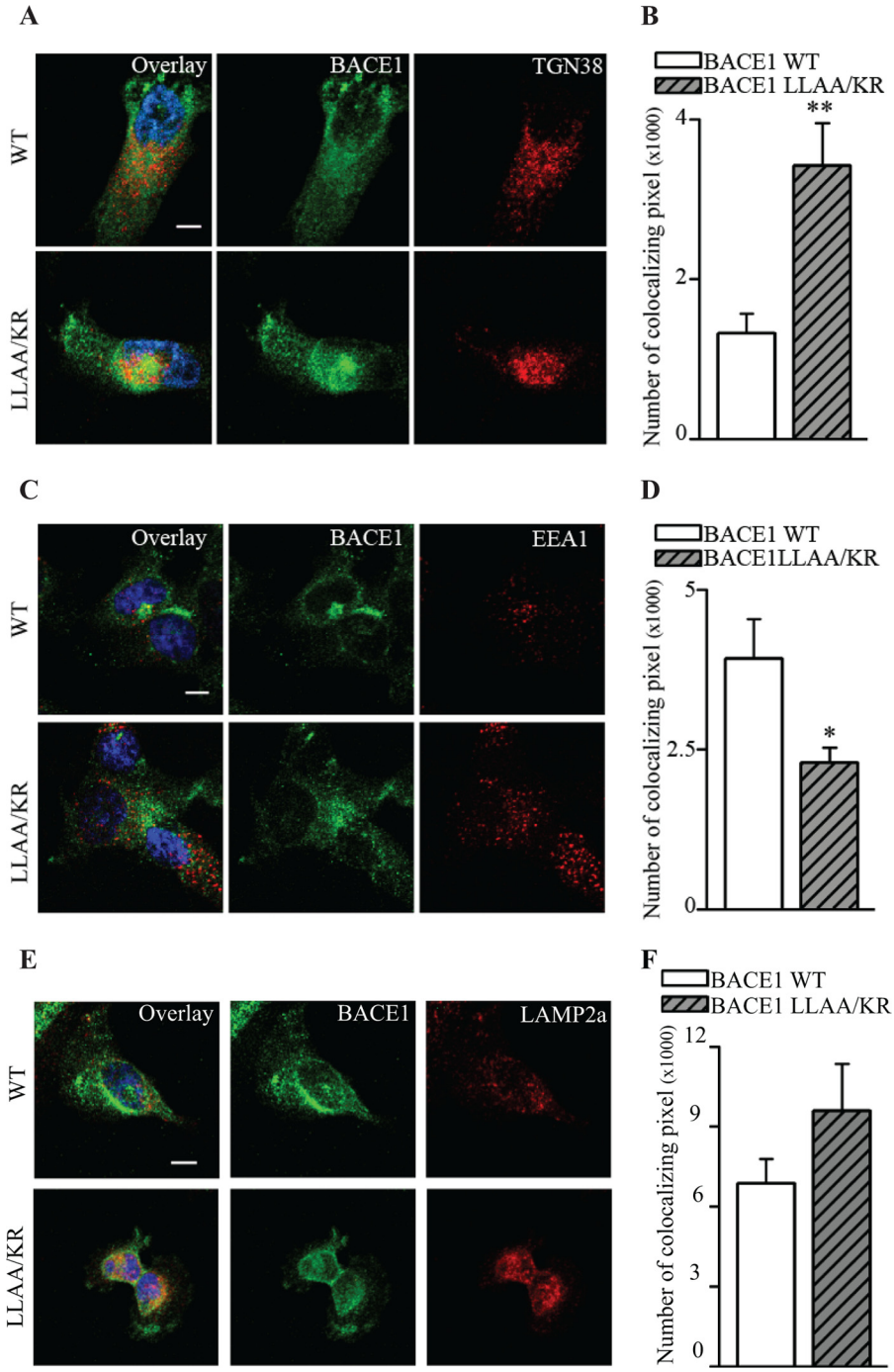

FIGURE 5. **Lack of ubiquitination and disruption of the di-leucine motif results in accumulation of BACE1 in TGN and reduction in early endosomes.** All *bar graphs* represent mean values of co-localizing pixels ± S.E. (**, $p < 0.001$; *, $p < 0.05$, one-way ANOVA), *scale bar,* 5 μm. *A,* representative photomicrographs of stable cell lines for BACE1WT (*upper lane*) and BACE1LLAA/KR (*lower lane*) stained with the trans-Golgi network marker TGN38. *B, bar graph* shows accumulation of BACE1LLAA/KR in the trans-Golgi network. *C,* representative photomicrographs of the same stable cell lines stained with the early endosomes marker EEA1. *D, bar graph* shows reduction of BACE1LLAA/KR in the early endosomes. *E,* representative photomicrographs of the same stable cell stained with the late endosomes/lysosomes marker LAMP2. *F, bar graph* shows no significant difference in accumulation of WT and mutant in the late endosomes/lysosomes.

several studies have shown that cargo proteins can be recruited in the GGA pathway not only via the di-leucine sorting motif but also via ubiquitin binding (29–33). The sorting and lysosomal degradation of cell membrane proteins (*e.g.* EGFR) are regulated by ubiquitination of critical lysines in their cytoplasmic domain (46, 47). Ubiquitinated EGFR, for instance, is sorted into vesicles that bud from the limiting membrane into the lumen of endosomes during the biogenesis of MVBs. Multivesicular bodies are considered to be late endosomes, formed from early endosomes by membrane invaginations that generate the inner vesicles with a lower pH (~5.5) (48).

Cargo selection during MVB sorting is dependent on several endosomal protein complexes required for transport (ESCRT). Several of these ESCRT components contain ubiquitin binding domains that act as receptors for ubiquitinated cargoes. For instance, ESCRT-0 consists of HRS and STAM, which contain Ub-interacting motifs. The tumor susceptibility gene (TSG101), a ubiquitin-binding subunit of ESCRT complex I, also contains a Ub-binding domain. Ubiquitinated cargoes are passed sequentially from ESCRT-0 to ESCRT-I and to ESCRT-II for final deposit into the forming luminal vesicles (for review see Ref. 36). Depletion of the endosomal proteins HRS, STAM1, STAM2, or TSG101 produces accumulation of EGFR in early endosomes (49–52).

Similarly, RNAi silencing of GGA3, but not GGA1 or GGA2, results in the accumulation of EGFR in enlarged early endosomes and partially blocks its delivery to lysosomes where it is normally degraded (29). The GGA3 GAT domain has also been shown to bind ubiquitin and TSG101 (29). Two ubiquitin-binding sites have been identified in the GGA3 GAT domain (53–55). One of these, site 2, centers on Leu-276. Substitution of L276A in the GGA3 GAT domain abrogates binding to ubiquitin and to TSG101 in a yeast two-hybrid system and results in the accumulation of EGFR in early endosomes upon expression in mammalian cells (29). Thus, GGA3 is able to bind Ub cargoes and transfer them to TSG101, functioning like HRS. It still needs to be determined whether GGA3 functions as ESCRT-0, alternatively or in parallel, with HRS.

We recently reported that GGA3 regulates BACE1 degradation independently of the VHS/di-leucine motif interaction but

TABLE 2

Percentage of BACE1 in different subcellular compartments

Values represent average numbers of co-localizing pixels ± S.E. NS means not significant.

	BACE1WT2	BACE1LLAA/KR	Statistics
TGN38	1318 ± 290	3416 ± 534**	**, $p = 0.0013$
Calnexin	1991 ± 360	2587 ± 332	NS
GM130	1436 ± 180	2095 ± 351	NS
EEA1	3925 ± 611	2293 ± 235*	*, $p = 0.018$
LAMP2	6875 ± 903	9590 ± 1699	NS

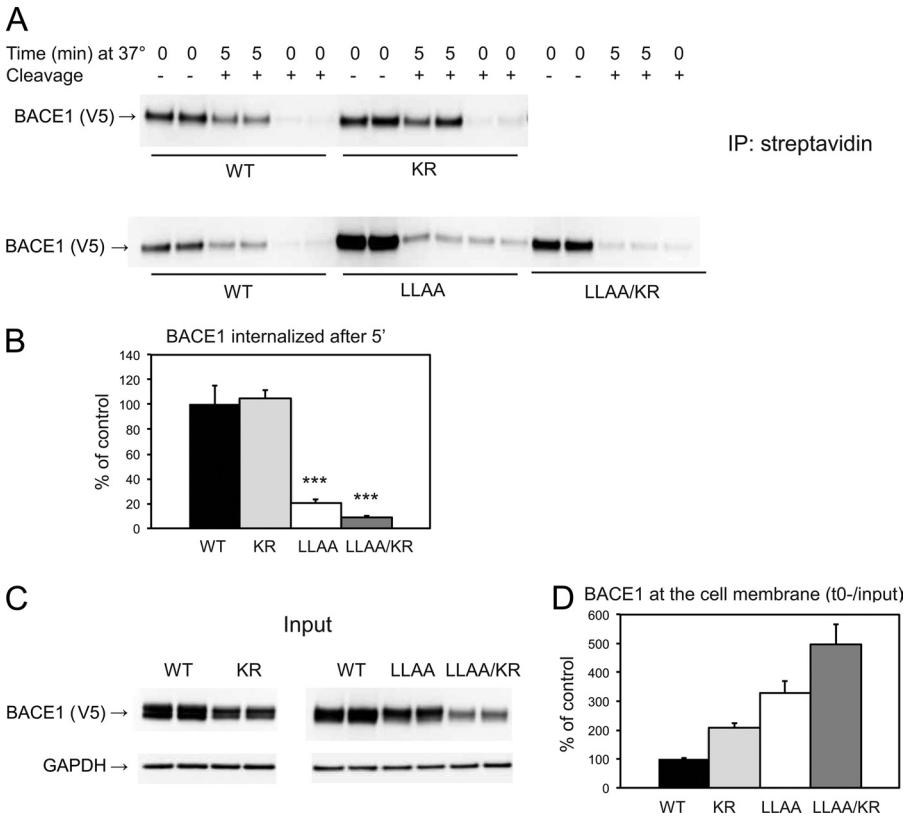

FIGURE 6. **Carboxyl-terminal di-leucine motif but not ubiquitination at Lys-501 regulates BACE1 endocytosis.** *A,* rate of BACE1 endocytosis analyzed via cell-surface biotinylation and pulldown with streptavidin beads. Levels of BACE1 were analyzed by WB using anti-V5 antibody. *B, bar graph* represents mean ± S.E. of at least three experiments. Internalization rates of BACE1KR were similar to BACE1WT, whereas BACE1LLAA and BACE1LLAA/KR exhibited significant defect as compared with WT. ***, $p < 0.001$, one-way ANOVA. *C,* Western blot analysis with anti-V5 and anti-GAPDH antibodies detected BACE1 levels in total lysates (*input*). *D, bar graph* represents mean ± S.E. of at least three experiments. Measurements of BACE1 pulled down without cleavage at *T*(0) were normalized against total BACE1 levels (*input*) from cell lysates to determine BACE1 levels at the cell membrane. Compared with BACE1WT, BACE1KR accumulated ~2-fold, whereas it was ~3.5-fold for BACE1LLAA and ~5-fold for BACE1LLAA/KR.

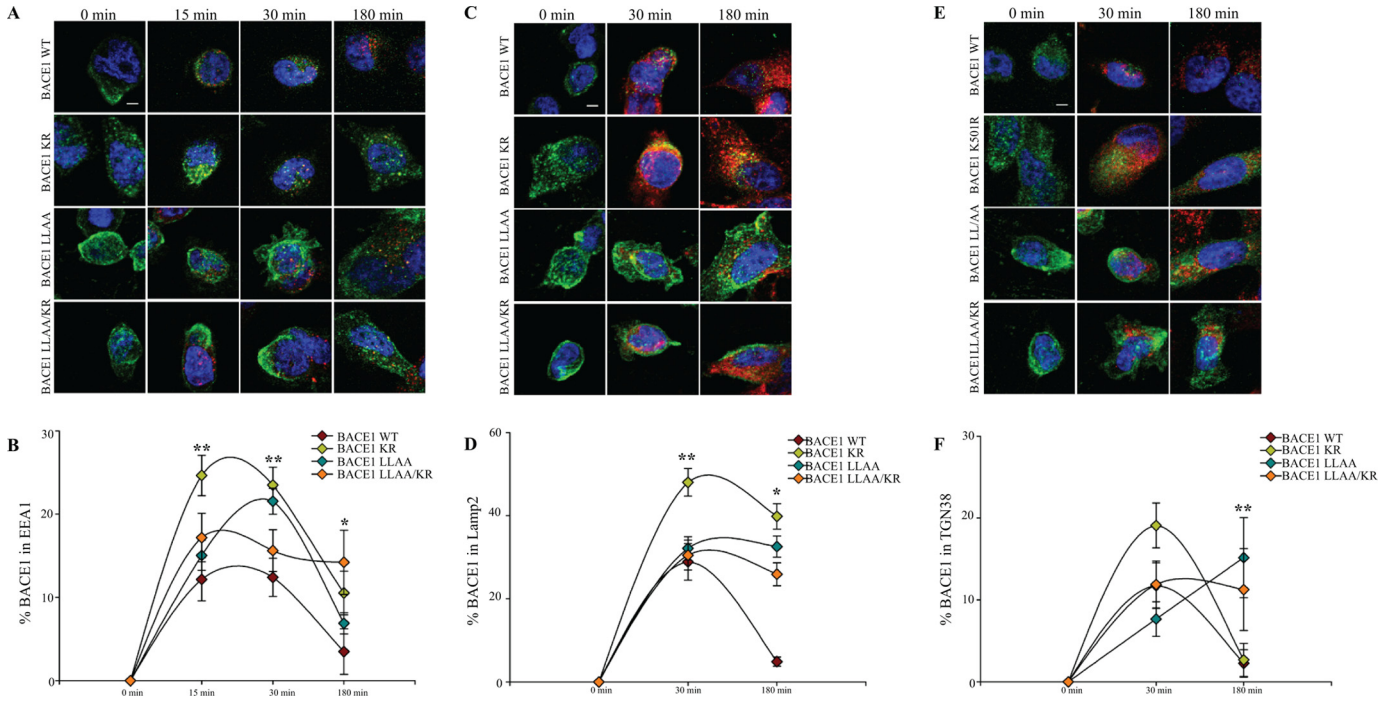

FIGURE 7. **Disruption of di-leucine motif delays trafficking to early and late endosomes/lysosomes and retrotransport to TGN following endocytosis.** All *line graphs* represent mean values of co-localizing pixels ±S.E. (**, $p < 0.001$; *, $p < 0.05$, one-way ANOVA), *scale bar*, 5 μm. All three stainings show a clear retention of BACE1LLAA and BACE1LLAA/KR at the cell membrane. *A,* representative photomicrographs of BACE1WT, BACE1KR, BACE1LLAA, and BACE1LLAA/KR after 15, 30, and 180 min of internalization and stained with the early endosomes marker EEA1. *B, line graph* shows accumulation of BACE1LLAA and BACE1LLAA/KR in the early endosomes after 30 and 180 min internalization, respectively. *C,* representative photomicrographs of BACE1WT, BACE1KR, BACE1LLAA, and BACE1LLAA/KR after 15, 30, and 180 min of internalization and stained with the late endosomes/lysosomes marker LAMP2. *D, line graph* shows accumulation of BACE1LLAA and BACE1LLAA/KR in the late endosomes and lysosomes after 180 min of internalization. *E,* representative photomicrographs of BACE1WT, BACE1KR, BACE1LLAA, and BACE1LLAA/KR after 15, 30, and 180 min of internalization and stained with the trans-Golgi network marker TGN38. *F, line graph* shows delayed transport of BACE1LLAA and BACE1LLAA/KR to the trans-Golgi network.

TABLE 3

Percentage of BACE1 in EEA1-positive compartments

Values represent average numbers of co-localizing pixels ±S.E.

	BACE1WT	BACE1KR	BACE1LLAA	BACE1LLAA/KR	Statistics
*T*15	12.16 ± 3	25.00 ± 2**	15.00 ± 2*	17.00 ± 3	**, $p = 0.0007$ *versus* WT; *, $p = 0.0079$ *versus* KR
*T*30	12.41 ± 2	23.50 ± 2**	21.54 ± 2*	15.62 ± 3	**, $p = 0.0006$ *versus* WT; *, $p = 0.0040$ *versus* WT
*T*180	3.49 ± 3	10.52 ± 3	6.88 ± 1	14.21 ± 4*	*, $p = 0.0092$ *versus* WT

TABLE 4

Percentage of BACE1 in LAMP2-positive compartments

Values represent average numbers of co-localizing pixels ±S.E.

	BACE1WT	BACE1KR	BACE1LLAA	BACE1LLAA/KR	Statistics
T 30	28.87 ± 4	48.03 ± 3***	31.16 ± 3**	30.51 ± 4*	***, $p = 0.0004$ *versus* WT; **, $p = 0.0028$ *versus* KR; *, $p = 0.001$ *versus* KR
T 180	4.86 ± 1	39.85 ± 3**	32.57 ± 3**	25.93 ± 3**$	**, $p < 0.001$ *versus* WT; $, $p = 0.002$ *versus* KR

TABLE 5

Percentage of BACE1 in TGN38-positive compartments

Values represent average numbers of co-localizing pixels ±S.E.

	BACE1WT	BACE1KR	BACE1LLAA	BACE1LLAA/KR	Statistics
T 30	11.74 ± 3	19.10 ± 3**	7.67 ± 2	11.88 ± 3	**, $p = 0.0036$ *versus* LLAA
T 180	2.25 ± 2	2.68 ± 2*	15.17 ± 5**	11.26 ± 5	**, $p = 0.0178$ *versus* WT; *, $p = 0.0217$ *versus* LLAA

requires binding to ubiquitin (35). In the same study we determined that BACE1 is ubiquitinated at Lys-501 and is mainly mono- and Lys-63-linked poly-ubiquitinated suggesting a role for BACE1 ubiquitination in endocytosis and sorting to the lysosomes for degradation (35). Our current data support a role of ubiquitination in sorting BACE1 to the lysosomes for degradation but not in BACE1 endocytosis. In contrast, the di-leucine motif is the major sorting signal for BACE1 internalization, trafficking to the lysosomes, and retrotransport to the TGN. Our present data indicate that BACE1 ubiquitination at Lys-501 or the presence of a functional di-leucine motif are sufficient for trafficking BACE1 from TGN to early endosomes. However, when both signals are disrupted, BACE1 accumulates in the TGN.

While this manuscript was in preparation, two reports were published supporting our findings. The first report

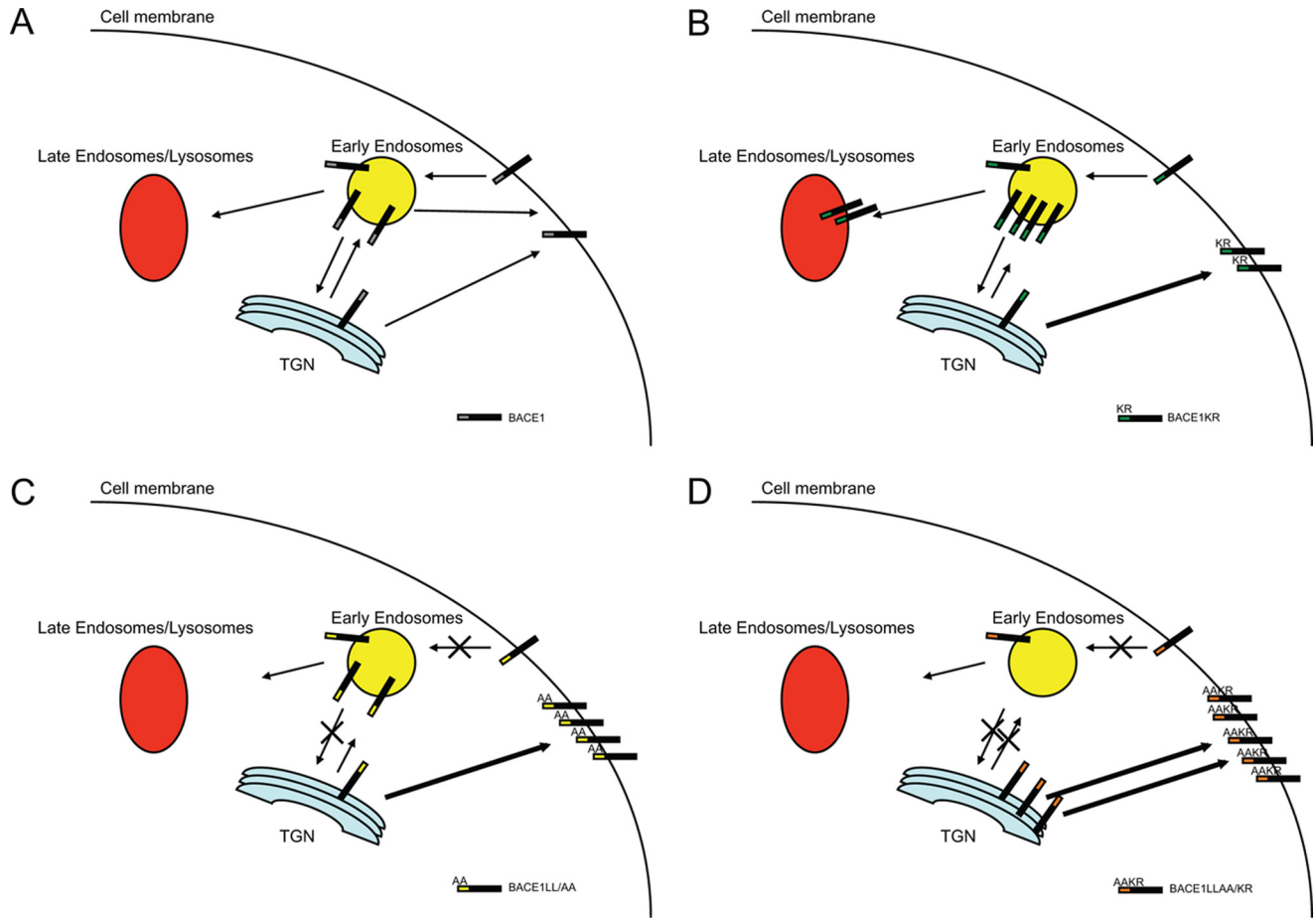

FIGURE 8. **Schematic representation of trafficking of normal and mutant BACE1.** *A,* BACE1 is normally trafficked from the TGN to the endosomes or directly to the cell membrane. After internalization in the endosomes is either transported to the late endosomes/lysosomes for degradation or retrotransported to the TGN. *B,* mutagenesis of the ubiquitination site at Lys-501 results in accumulation of BACE1 at the cell membrane and the early and late endosomes/lysosomes. Internalization rate does not appear to be affected. *C,* disruption of di-leucine motif results in retention of BACE1 at the cell membrane and a delay in retrotransport of BACE1 to the TGN. Passage to the lysosomes is also postponed thus impairing degradation of BACE1. *D,* disruption of both the Lys-501 ubiquitination site and the di-leucine motif causes an accumulation of BACE1 in the TGN and decreases levels in the early endosomes indicating a failure in passage from the TGN to the endosomes. Compared with the single mutants, BACE1LLAA/KR retention at the cell membrane is significantly higher and may be attributed to direct passage of BACE1 to the cell membrane having circumvented transportation to the endosomes.

showed that the di-leucine motif mediates the interaction with the retromer complex, which regulates BACE1 retrotransport to the TGN (56). The second report determined that the ^{494}DISLL^{500} sequence in BACE1 CTF is embedded within a longer (DE)*XXX*L(LI) sequence that interacts with AP-2 regulating its endocytosis, whereas siRNA-mediated knockdown of AP-1 has no effect on BACE1 intracellular localization (57). Given that AP-1 and GGAs are the adaptor proteins that regulate the trafficking of cargoes between the TGN and the endosomes, these new findings further confirm the key role of GGAs in the trafficking of BACE1 between these two compartments.

Taking all these findings together, we can hypothesize that GGAs may play a dual role in the trafficking of BACE1. It is possible that GGAs traffic BACE1 from the TGN to early endosomes (44). Then BACE1 is transported from the endosomes to the cell membrane, where it can be internalized to the endosomes again. At this point, GGAs can transport BACE1 back to the TGN (26) or sort it to the lysosomes for degradation. Given our previous and current data, we can hypothesize that GGA3 traffics ubiquitinated BACE1 from the TGN to endosomes and from endosomes to lysosomes and that GGA1 and GGA2 regulate BACE1 transport from the TGN to the endosomes, and vice versa, via interaction with the di-leucine motif. Further studies will be necessary to determine whether GGAs play different roles in the trafficking of BACE1.

In summary, our studies have determined that BACE1 ubiquitination regulates BACE1 degradation but not its endocytosis. Thus, drugs able to increase BACE1 ubiquitination in the brain will result in increased BACE1 degradation without favoring BACE1 internalization to the endosomes and the subsequent Aβ generation. Given that decreasing BACE1 levels represent an alternative approach to BACE1 direct inhibition, therapies able to increase BACE1 ubiquitination may represent a potential treatment for AD.

Acknowledgments—We thank Dr. Kendall Walker for the useful comments in the preparation and editing of this manuscript. We thank Dr. Alenka Lovy-Wheeler of the Tufts Imaging Facility for help with confocal microscopy (Tufts Center for Neuroscience Research, supported by National Institutes of Health Grant P30 NS047243).

REFERENCES

1. Vassar, R., Bennett, B. D., Babu-Khan, S., Kahn, S., Mendiaz, E. A., Denis, P., Teplow, D. B., Ross, S., Amarante, P., Loeloff, R., Luo, Y., Fisher, S., Fuller, J., Edenson, S., Lile, J., Jarosinski, M. A., Biere, A. L., Curran, E., Burgess, T., Louis, J. C., Collins, F., Treanor, J., Rogers, G., and Citron, M. (1999) β-Secretase cleavage of Alzheimer amyloid precursor protein by the transmembrane aspartic protease BACE. *Science* **286,** 735–741
2. Sinha, S., Anderson, J. P., Barbour, R., Basi, G. S., Caccavello, R., Davis, D., Doan, M., Dovey, H. F., Frigon, N., Hong, J., Jacobson-Croak, K., Jewett, N., Keim, P., Knops, J., Lieberburg, I., Power, M., Tan, H., Tatsuno, G., Tung, J., Schenk, D., Seubert, P., Suomensaari, S. M., Wang, S., Walker, D., Zhao, J., McConlogue, L., and John, V. (1999) Purification and cloning of amyloid precursor protein β-secretase from human brain. *Nature* **402,** 537–540
3. Yan, R., Bienkowski, M. J., Shuck, M. E., Miao, H., Tory, M. C., Pauley, A. M., Brashier, J. R., Stratman, N. C., Mathews, W. R., Buhl, A. E., Carter, D. B., Tomasselli, A. G., Parodi, L. A., Heinrikson, R. L., and Gurney, M. E. (1999) Membrane-anchored aspartyl protease with Alzheimer disease β-secretase activity. *Nature* **402,** 533–537
4. Hong, L., Koelsch, G., Lin, X., Wu, S., Terzyan, S., Ghosh, A. K., Zhang, X. C., and Tang, J. (2000) Structure of the protease domain of memapsin 2 (β-secretase) complexed with inhibitor. *Science* **290,** 150–153
5. Creemers, J. W., Ines Dominguez, D., Plets, E., Serneels, L., Taylor, N. A., Multhaup, G., Craessaerts, K., Annaert, W., and De Strooper, B. (2001) Processing of β-secretase by furin and other members of the proprotein convertase family. *J. Biol. Chem.* **276,** 4211–4217
6. Cai, H., Wang, Y., McCarthy, D., Wen, H., Borchelt, D. R., Price, D. L., and Wong, P. C. (2001) Bace1 is the major β-secretase for generation of Aβ peptides by neurons. *Nat. Neurosci.* **4,** 233–234
7. Luo, Y., Bolon, B., Kahn, S., Bennett, B. D., Babu-Khan, S., Denis, P., Fan, W., Kha, H., Zhang, J., Gong, Y., Martin, L., Louis, J. C., Yan, Q., Richards, W. G., Citron, M., and Vassar, R. (2001) Mice deficient in Bace1, the Alzheimer β-secretase, have normal phenotype and abolished β-amyloid generation. *Nat. Neurosci.* **4,** 231–232
8. Roberds, S. L., Anderson, J., Basi, G., Bienkowski, M. J., Branstetter, D. G., Chen, K. S., Freedman, S. B., Frigon, N. L., Games, D., Hu, K., Johnson-Wood, K., Kappenman, K. E., Kawabe, T. T., Kola, I., Kuehn, R., Lee, M., Liu, W., Motter, R., Nichols, N. F., Power, M., Robertson, D. W., Schenk, D., Schoor, M., Shopp, G. M., Shuck, M. E., Sinha, S., Svensson, K. A., Tatsuno, G., Tintrup, H., Wijsman, J., Wright, S., and McConlogue, L. (2001) Bace knockout mice are healthy despite lacking the primary β-secretase activity in brain. Implications for Alzheimer disease therapeutics. *Hum. Mol. Genet.* **10,** 1317–1324
9. McConlogue, L., Buttini, M., Anderson, J. P., Brigham, E. F., Chen, K. S., Freedman, S. B., Games, D., Johnson-Wood, K., Lee, M., Zeller, M., Liu, W., Motter, R., and Sinha, S. (2007) Partial reduction of BACE1 has dramatic effects on Alzheimer plaque and synaptic pathology in APP transgenic mice. *J. Biol. Chem.* **282,** 26326–26334
10. Ohno, M., Chang, L., Tseng, W., Oakley, H., Citron, M., Klein, W. L., Vassar, R., and Disterhoft, J. F. (2006) Temporal memory deficits in Alzheimer mouse models. Rescue by genetic deletion of Bace1. *Eur. J. Neurosci.* **23,** 251–260
11. Ohno, M., Cole, S. L., Yasvoina, M., Zhao, J., Citron, M., Berry, R., Disterhoft, J. F., and Vassar, R. (2007) BACE1 gene deletion prevents neuron loss and memory deficits in 5XFAD APP/PS1 transgenic mice. *Neurobiol. Dis.* **26,** 134–145
12. Ohno, M., Sametsky, E. A., Younkin, L. H., Oakley, H., Younkin, S. G., Citron, M., Vassar, R., and Disterhoft, J. F. (2004) Bace1 deficiency rescues memory deficits and cholinergic dysfunction in a mouse model of Alzheimer disease. *Neuron* **41,** 27–33
13. Willem, M., Garratt, A. N., Novak, B., Citron, M., Kaufmann, S., Rittger, A., DeStrooper, B., Saftig, P., Birchmeier, C., and Haass, C. (2006) Control of peripheral nerve myelination by the β-secretase BACE1. *Science* **314,** 664–666
14. Hu, X., Hicks, C. W., He, W., Wong, P., Macklin, W. B., Trapp, B. D., and Yan, R. (2006) Bace1 modulates myelination in the central and peripheral nervous system. *Nat. Neurosci.* **9,** 1520–1525
15. Savonenko, A. V., Melnikova, T., Laird, F. M., Stewart, K. A., Price, D. L., and Wong, P. C. (2008) Alteration of BACE1-dependent NRG1/ErbB4 signaling and schizophrenia-like phenotypes in BACE1-null mice. *Proc. Natl. Acad. Sci. U.S.A.* **105,** 5585–5590
16. Sankaranarayanan, S., Price, E. A., Wu, G., Crouthamel, M. C., Shi, X. P., Tugusheva, K., Tyler, K. X., Kahana, J., Ellis, J., Jin, L., Steele, T., Stachel, S., Coburn, C., and Simon, A. J. (2008) *In vivo* β-secretase 1 inhibition leads to brain Aβ lowering and increased α-secretase processing of amyloid precursor protein without effect on neuregulin-1. *J. Pharmacol. Exp. Ther.* **324,** 957–969
17. De Strooper, B. (2010) Proteases and proteolysis in Alzheimer disease. A multifactorial view on the disease process. *Physiol. Rev.* **90,** 465–494
18. He, W., Lu, Y., Qahwash, I., Hu, X. Y., Chang, A., and Yan, R. (2004) Reticulon family members modulate BACE1 activity and amyloid-β peptide generation. *Nat. Med.* **10,** 959–965
19. Vassar, R., Kovacs, D. M., Yan, R., and Wong, P. C. (2009) The β-secretase enzyme bace in health and Alzheimer disease: Regulation, cell biology, function, and therapeutic potential. *J. Neurosci.* **29,** 12787–12794
20. Bonifacino, J. S., and Traub, L. M. (2003) Signals for sorting of transmembrane proteins to endosomes and lysosomes. *Annu. Rev. Biochem.* **72,** 395–447
21. Huse, J. T., Pijak, D. S., Leslie, G. J., Lee, V. M., and Doms, R. W. (2000) Maturation and endosomal targeting of β-site amyloid precursor protein-cleaving enzyme. The Alzheimer disease β-secretase. *J. Biol. Chem.* **275,** 33729–33737
22. Pastorino, L., Ikin, A. F., Nairn, A. C., Pursnani, A., and Buxbaum, J. D. (2002) The carboxyl terminus of BACE contains a sorting signal that regulates BACE trafficking but not the formation of total A(β). *Mol. Cell. Neurosci.* **19,** 175–185
23. Koh, Y. H., von Arnim, C. A., Hyman, B. T., Tanzi, R. E., and Tesco, G. (2005) BACE is degraded via the lysosomal pathway. *J. Biol. Chem.* **280,** 32499–32504
24. Walter, J., Fluhrer, R., Hartung, B., Willem, M., Kaether, C., Capell, A., Lammich, S., Multhaup, G., and Haass, C. (2001) Phosphorylation regulates intracellular trafficking of β-secretase. *J. Biol. Chem.* **276,** 14634–14641
25. He, X., Zhu, G., Koelsch, G., Rodgers, K. K., Zhang, X. C., and Tang, J. (2003) Biochemical and structural characterization of the interaction of memapsin 2 (β-secretase) cytosolic domain with the vhs domain of GGA proteins. *Biochemistry* **42,** 12174–12180
26. Wahle, T., Prager, K., Raffler, N., Haass, C., Famulok, M., and Walter, J. (2005) GGA proteins regulate retrograde transport of BACE1 from endosomes to the trans-Golgi network. *Mol. Cell. Neurosci.* **29,** 453–461
27. von Arnim, C. A., Tangredi, M. M., Peltan, I. D., Lee, B. M., Irizarry, M. C., Kinoshita, A., and Hyman, B. T. (2004) Demonstration of BACE (β-secretase) phosphorylation and its interaction with GGA1 in cells by fluorescence-lifetime imaging microscopy. *J. Cell Sci.* **117,** 5437–5445
28. Shiba, T., Kametaka, S., Kawasaki, M., Shibata, M., Waguri, S., Uchiyama, Y., and Wakatsuki, S. (2004) Insights into the phosphoregulation of β-secretase sorting signal by the VHS domain of GGA1. *Traffic* **5,** 437–448
29. Puertollano, R., and Bonifacino, J. S. (2004) Interactions of GGA3 with the ubiquitin sorting machinery. *Nat. Cell Biol.* **6,** 244–251
30. Scott, P. M., Bilodeau, P. S., Zhdankina, O., Winistorfer, S. C., Hauglund, M. J., Allaman, M. M., Kearney, W. R., Robertson, A. D., Boman, A. L., and Piper, R. C. (2004) GGA proteins bind ubiquitin to facilitate sorting at the trans-Golgi network. *Nat. Cell Biol.* **6,** 252–259
31. Pak, Y., Glowacka, W. K., Bruce, M. C., Pham, N., and Rotin, D. (2006) Transport of LAPTM5 to lysosomes requires association with the ubiquitin ligase Nedd4, but not LAPTM5 ubiquitination. *J. Cell Biol.* **175,** 631–645
32. Lauwers, E., Jacob, C., and André, B. (2009) Lys-63-linked ubiquitin chains as a specific signal for protein sorting into the multivesicular body pathway. *J. Cell Biol.* **185,** 493–502
33. Deng, Y., Guo, Y., Watson, H., Au, W. C., Shakoury-Elizeh, M., Basrai, M. A., Bonifacino, J. S., and Philpott, C. C. (2009) GGA2 mediates sequential ubiquitin-independent and ubiquitin-dependent steps in the trafficking of ARN1 from the trans-Golgi network to the vacuole. *J. Biol. Chem.*

284, 23830–23841
34. Tesco, G., Koh, Y. H., Kang, E. L., Cameron, A. N., Das, S., Sena-Esteves, M., Hiltunen, M., Yang, S. H., Zhong, Z., Shen, Y., Simpkins, J. W., and Tanzi, R. E. (2007) Depletion of GGA3 stabilizes BACE and enhances β-secretase activity. *Neuron* **54,** 721–737
35. Kang, E. L., Cameron, A. N., Piazza, F., Walker, K. R., and Tesco, G. (2010) Ubiquitin regulates GGA3-mediated degradation of BACE1. *J. Biol. Chem.* **285,** 24108–24119
36. Piper, R. C., and Luzio, J. P. (2007) Ubiquitin-dependent sorting of integral membrane proteins for degradation in lysosomes. *Curr. Opin. Cell Biol.* **19,** 459–465
37. Davies, B. A., Lee, J. R., Oestreich, A. J., and Katzmann, D. J. (2009) Membrane protein targeting to the MVB/lysosome. *Chem. Rev.* **109,** 1575–1586
38. Mukhopadhyay, D., and Riezman, H. (2007) Proteasome-independent functions of ubiquitin in endocytosis and signaling. *Science* **315,** 201–205
39. Lauwers, E., Erpapazoglou, Z., Haguenauer-Tsapis, R., and Andre, B. (2010) The ubiquitin code of yeast permease trafficking. *Trends Cell Biol.* **20,** 196–204
40. Ren, X., and Hurley, J. H. (2010) VHS domains of ESCRT-0 cooperate in high-avidity binding to polyubiquitinated cargo. *EMBO J.* **29,** 1045–1054
41. Jaskolski, F., Mulle, C., and Manzoni, O. J. (2005) An automated method to quantify and visualize colocalized fluorescent signals. *J. Neurosci. Methods* **146,** 42–49
42. Liu, K., Doms, R. W., and Lee, V. M. (2002) Glu11 site cleavage and N-terminally truncated a β production upon BACE overexpression. *Biochemistry* **41,** 3128–3136
43. Katzmann, D. J., Babst, M., and Emr, S. D. (2001) Ubiquitin-dependent sorting into the multivesicular body pathway requires the function of a conserved endosomal protein sorting complex, ESCRT-I. *Cell* **106,** 145–155
44. He, X., Li, F., Chang, W. P., and Tang, J. (2005) GGA proteins mediate the recycling pathway of memapsin 2 (BACE). *J. Biol. Chem.* **280,** 11696–11703
45. Sannerud, R., Declerck, I., Peric, A., Raemaekers, T., Menendez, G., Zhou, L., Veerle, B., Coen, K., Munck, S., De Strooper, B., Schiavo, G., and Annaert, W. (2011) ADP ribosylation factor 6 (ARF6) controls amyloid precursor protein (APP) processing by mediating the endosomal sorting of BACE1. *Proc. Natl. Acad. Sci. U.S.A.* **108,** E559–E568
46. Longva, K. E., Blystad, F. D., Stang, E., Larsen, A. M., Johannessen, L. E., and Madshus, I. H. (2002) Ubiquitination and proteasomal activity is required for transport of the EGF receptor to inner membranes of multivesicular bodies. *J. Cell Biol.* **156,** 843–854
47. Huang, F., Kirkpatrick, D., Jiang, X., Gygi, S., and Sorkin, A. (2006) Differential regulation of EGF receptor internalization and degradation by multi-ubiquitination within the kinase domain. *Mol. Cell* **21,** 737–748
48. Gruenberg, J. (2001) The endocytic pathway. A mosaic of domains. *Nat. Rev. Mol. Cell Biol.* **2,** 721–730
49. Bache, K. G., Brech, A., Mehlum, A., and Stenmark, H. (2003) Hrs regulates multivesicular body formation via escrt recruitment to endosomes. *J. Cell Biol.* **162,** 435–442
50. Bache, K. G., Raiborg, C., Mehlum, A., and Stenmark, H. (2003) STAM and Hrs are subunits of a multivalent ubiquitin-binding complex on early endosomes. *J. Biol. Chem.* **278,** 12513–12521
51. Bishop, N., Horman, A., and Woodman, P. (2002) Mammalian class E vps proteins recognize ubiquitin and act in the removal of endosomal protein-ubiquitin conjugates. *J. Cell Biol.* **157,** 91–101
52. Lu, Q., Hope, L. W., Brasch, M., Reinhard, C., and Cohen, S. N. (2003) TSG101 interaction with HRS mediates endosomal trafficking and receptor down-regulation. *Proc. Natl. Acad. Sci. U.S.A.* **100,** 7626–7631
53. Bilodeau, P. S., Winistorfer, S. C., Allaman, M. M., Surendhran, K., Kearney, W. R., Robertson, A. D., and Piper, R. C. (2004) The GAT domains of clathrin-associated GGA proteins have two ubiquitin binding motifs. *J. Biol. Chem.* **279,** 54808–54816
54. Prag, G., Lee, S., Mattera, R., Arighi, C. N., Beach, B. M., Bonifacino, J. S., and Hurley, J. H. (2005) Structural mechanism for ubiquitinated-cargo recognition by the Golgi-localized, γ-ear-containing, ADP-ribosylation-factor-binding proteins. *Proc. Natl. Acad. Sci. U.S.A.* **102,** 2334–2339
55. Kawasaki, M., Shiba, T., Shiba, Y., Yamaguchi, Y., Matsugaki, N., Igarashi, N., Suzuki, M., Kato, R., Kato, K., Nakayama, K., and Wakatsuki, S. (2005) Molecular mechanism of ubiquitin recognition by GGA3 GAT domain. *Genes Cells* **10,** 639–654
56. Cuartero, Y., Mellado, M., Capell, A., Alvarez-Dolado, M., and Verges, M. (2012) Retromer regulates postendocytic sorting of ss-secretase in polarized Madin-Darby canine kidney cells. *Traffic* **13,** 1393–1410
57. Prabhu, Y., Burgos, P. V., Schindler, C., Farías, G. G., Magadán, J. G., and Bonifacino, J. S. (2012) Adaptor protein 2-mediated endocytosis of the β-secretase BACE1 is dispensable for amyloid precursor protein processing. *Mol. Biol. Cell* **23,** 2339–2351